Pricing in affine forward variance models

Jim Gatheral

BaruchCOLLEGE
WEISSMAN SCHOOL OF ARTS AND SCIENCES

**Master of
Financial
Engineering**

Seminario di finanza matematica, probabilità
Bologna, October 13, 2021

Outline of this talk

- Affine forward variance (AFV) models
  - The classical Heston model
  - The rough Heston model
- The CGF and its associated Volterra integral equation
  - Numerical solution using the Adams scheme
  - Rational approximation of the rough Heston solution
- Simulation of AFV models
  - The RSQE scheme
  - The HQE scheme
  - Convergence

Forward variance models

- Let S be a strictly positive continuous martingale.

- Then $X := \log S$ is a semimartingale with quadratic variation process $\langle X \rangle$.

- Following [BG12], it is natural to specify a model in forward variance form.

$$
\begin{aligned}
v_t \, dt &:= d\langle X \rangle_t \\
\xi_t(T) &= \mathbb{E}\left[v_T | \mathcal{F}_t \right].
\end{aligned}
$$

  - Forward variances are tradable assets (unlike spot variance).
  - We get a family of martingales indexed by their individual time horizons T.

- As noted in [BG12], all conventional finite-dimensional Markovian stochastic volatility models may be cast as forward variance models.

Example: The classical Heston model

The classical Heston stochastic volatility model may be written as

$$
\begin{aligned}
\frac{dS_t}{S_t} &= \sqrt{v_t}\, dZ_t \\
dv_t &= -\lambda\,(v_t - \bar{v})\, dt + \eta\,\sqrt{v_t}\, dW_t
\end{aligned}
$$

with $\mathbb{E}\,[dZ_t\, dW_t] = \rho\, dt$ and where λ is the speed of reversion of v_t to its long term mean $\bar{v}$.

Forward variance in the Heston model

With $\xi_t(u) = \mathbb{E}\left[v_u | \mathcal{F}_t \right]$, take expectations of the SDE for v_t to get

$$d\xi_t(u) = -\lambda \left(\xi_t(u) - \bar{v} \right) du.$$

This ODE has the solution

$$\xi_t(u) = \left(\xi_t(t) - \bar{v} \right) e^{-\lambda (u-t)} + \bar{v} = \left(v_t - \bar{v} \right) e^{-\lambda (u-t)} + \bar{v}.$$

The Heston model in forward variance form

For each fixed u, $\xi_t(u)$ is a conditional expectation and so a martingale in t. It is then immediate from the last equation that

Classical Heston

$$d\xi_t(u) = \eta \, e^{-\lambda \, (u-t)} \sqrt{v_t} \, dW_t$$

- It is easy to check explicitly that all drift (*i.e. dt) terms cancel.*

Affine CGF

Let $X_t = \log S_t$. According to Definition 2.2 of [GKR19], a forward variance model has an *affine cumulant generating function* determined by $g(t; u)$, if its conditional cumulant generating function is of the form

$$\log \mathbb{E}\left[\left. e^{u(X_T - X_t)} \right| \mathcal{F}_t \right] = \int_t^T \xi_t(s)\, g(T - s; u)\, ds. \qquad (1)$$

When is a forward variance model affine?

Theorem 2.4 of [GKR19] states that a forward variance model has an affine CGF if and only if it takes the form

$$
\begin{aligned}
\frac{dS_t}{S_t} &= \sqrt{v_t}\, dZ_t \\
d\xi_t(u) &= \kappa(u - t)\sqrt{v_t}\, dW_t
\end{aligned}
$$

for some deterministic, non-negative decreasing kernel κ, which satisfies $\int_0^T \kappa(r)dr < \infty$ for all $T > 0$.

- Essentially, the only affine stochastic volatility model is the Heston model, up to a choice of kernel.

Another example: Rough Heston

With $\alpha = H + 1/2 \in (1/2, 1)$, the rough Heston model of [ER19] reads

$$v_u = \theta_t(u) - \frac{1}{\Gamma(\alpha)} \int_t^u (u-s)^{\alpha-1} \lambda\, v_s\, ds + \frac{1}{\Gamma(\alpha)} \int_t^u (u-s)^{\alpha-1} \nu \sqrt{v_s}\, dW_s.$$

In the special case $\lambda = 0$, this model takes the forward variance form (again by inspection):

Rough Heston

'

$$d\xi_t(u) = \frac{\nu}{\Gamma(\alpha)}\, (u - t)^{\alpha-1} \sqrt{v_t}\, dW_t.$$

Solving for $g(\cdot)$

$g(\cdot; u)$ in the definition (1) of the CGF is the unique global continuous solution of the convolution Riccati equation

$$
g(\tau; u) = R_V\Big(u, \int_0^\tau \kappa(\tau - s) g(s; u) ds\Big) = R_V\Big(u, (\kappa \star g)(\tau; u)\Big)
$$

(2)

where

$$
R_V(u, w) = \frac{1}{2}(u^2 - u) + \rho\, u\, w + \frac{1}{2}\, w^2.
$$

An aside: Fractional calculus

Define the fractional integral and differential operators:

$$I^\alpha f(t) = \frac{1}{\Gamma(\alpha)} \int_0^t (t-s)^{\alpha-1} f(s)\, ds; \quad D^\alpha f(t) = \frac{d}{dt}\, I^{1-\alpha} f(t).$$

The fractional integral is a natural generalization of the ordinary integral using the Cauchy formula for repeated integration:

$$\begin{aligned}
I^n f(t) &:= \int_0^t dt_1 \int_0^{t_1} ... dt_{n-1} \int_0^{t_{n-1}} f(t_n)\, dt_n \\
&= \frac{1}{(n-1)!} \int_0^t (t-s)^{n-1} f(s)\, ds.
\end{aligned}$$

Convolution Riccati equation as a fractional ODE

- When the kernel is of the form $\kappa(\tau) \sim \tau^{\alpha-1}$, the convolution Riccati equation may be rewritten as a fractional ODE.
- For example, in the case of the rough Heston model (with $\lambda = 0$), with $\alpha = H + \frac{1}{2}$,

$$
\begin{aligned}
\nu\, h(\tau; u) &:= (\kappa \star g)(\tau; u) \\
&= \frac{\eta}{\Gamma(\alpha)} \int_0^\tau (\tau - s)^{\alpha-1}\, g(s; u)\, ds \\
&= \nu\, I^\alpha g(\tau; u).
\end{aligned}
$$

- Inverting this gives $g(\tau; u) = D^\alpha h(\tau; u)$.

Convolution Riccati equation as a fractional ODE

The convolution integral Riccati equation then reads

$$D^{\alpha} h(\tau; u) = \frac{1}{2} u (u-1) + \rho \nu u h(\tau; u) + \frac{1}{2} \nu^2 h(\tau; u)^2, \qquad (3)$$

consistent with [ER19].

Computing option prices from the characteristic function

- It is quite straightforward to get option prices by inverting the characteristic function of a given stochastic process (if it is known in closed-form).
- For example, formula (5.6) of [Gat06] is a special case of formula (2.10) of [Lew00]:

Lemma 1 (Formula (2.10) of Lewis)

$$C(S, K, t, T) = S - \sqrt{SK} \frac{1}{\pi} \int_0^\infty \frac{du}{u^2 + \frac{1}{4}} \operatorname{Re} \left[e^{-iuk} \varphi_t \left(T; u - i/2 \right) \right]$$

with $k = \log \left(\frac{K}{S} \right)$.

- An analogous formula holds for puts.

Alternative methods

Alternative methods include:

- The COS method of [FO09]
- The SINC method of [BBRR21].
- Both of these methods, in particular the SINC method, are significantly faster and more accurate than the Lewis formula when calculating the prices of many options with the same expiration.
    - *i.e.* when computing smiles.

Summary so far

- Given the characteristic function, it is straightforward to price European options.
- In AFV models, the characteristic function is given by

$$\mathbb{E}_t\left[e^{iaX_T}\right] =: \varphi_t(T; a) = \exp\left\{\int_t^T \xi_t(s)\, g(T - s; ia)\, ds\right\}$$

where $g(\cdot; u)$ is the unique global continuous solution of the convolution Riccati equation (2):

$$g(\tau; u) = R_V\Big(u, (\kappa \star g)(\tau, u)\Big),$$

and $R_V(u, w) = \frac{1}{2}(u^2 - u) + \rho\, u\, w + \frac{1}{2}\, w^2$.

- All we therefore need to do is to solve (2).

The fractional Adams scheme

The fractional Adams scheme of [DFF04] is for the numerical approximation of the solution of equations of the form

$$h(\tau) = \frac{1}{\Gamma(\alpha)} \int_0^\tau (\tau - s)^{\alpha - 1} F(h(s)) \, ds. \tag{4}$$

- The rough Heston convolution Riccati equation is of this type.

The idea is as follows. Write $g(t) = F(h(t))$. With a regular grid $\Delta = \tau/n$, $0 = t_0 < t_1 < \ldots \leq t_n = \tau$, we approximate

$$h(t_{k+1}) = \frac{1}{\Gamma(\alpha)} \int_0^{t_{k+1}} (t_{k+1} - s)^{\alpha-1} g(s) \, ds$$

by

$$\frac{1}{\Gamma(\alpha)} \int_0^t (t - s)^{\alpha-1} \hat{g}(s) \, ds,$$

where $\hat{g}$ is the linear interpolation of g:

$$\hat{g}(t) = \frac{t_{j+1} - t}{t_{j+1} - t_j} \hat{g}(t_j) + \frac{t - t_j}{t_{j+1} - t_j} \hat{g}(t_{j+1}), \ \ t \in [t_j, t_{j+1}], \ \ 0 \leq j \leq k.$$

This leads to the following scheme:

$$\hat{h}(t_{k+1}) = \sum_{0 \leq j \leq k} a_{j,k+1} F(\hat{h}(t_j)) + a_{k+1,k+1} F(\hat{h}(t_{k+1})), \quad (5)$$

with

$$
\begin{aligned}
a_{0,k+1} &= \frac{\Delta^{\alpha}}{\Gamma(\alpha+2)}[k^{\alpha+1} - (k-\alpha)(k+1)^{\alpha}] \\
a_{j,k+1} &= \frac{\Delta^{\alpha}}{\Gamma(\alpha+2)}[(k-j+2)^{\alpha+1} + (k-j)^{\alpha+1} - 2(k-j+1)^{\alpha+1}]; \\
&\quad 1 \leq j \leq k \\
a_{k+1,k+1} &= \frac{(\Delta t)^{\alpha}}{\Gamma(\alpha+2)}. \quad (6)
\end{aligned}
$$

- $\hat{h}(t_{k+1})$ is on both sides of (5) so this scheme is implicit.
- Thus, we first compute a predictor of $\hat{h}^P(t_{k+1})$ of $\hat{h}(t_{k+1})$ and plug that predictor back into (5).
- We construct the predictor $\hat{h}^P(t_{k+1})$ by freezing $\hat{g}$ at the beginning of each interval:

$$\hat{h}^P(t_{k+1}) = \frac{1}{\Gamma(\alpha)} \int_0^{t_{k+1}} (t_{k+1} - s)^{\alpha-1} \tilde{g}(s) ds,$$

with

$$\tilde{g}(t) = \hat{g}(t_j); \quad t \in [t_j, t_{j+1}), \quad 0 \le j \le k.$$

Therefore,

$$\hat{h}^P(t_{k+1}) = \sum_{0 \leq j \leq k} b_{j,k+1} F\big(\hat{h}(t_j)\big),$$

where

$$b_{j,k+1} = \frac{\Delta^\alpha}{\Gamma(\alpha+1)} \left[(k-j+1)^\alpha - (k-j)^\alpha\right], \ \ 0 \leq j \leq k.$$

Thus, the final explicit numerical scheme is given by

$$\hat{h}(t_{k+1}) = \sum_{0 \leq j \leq k} a_{j,k+1} F(\hat{h}(t_j)) + a_{k+1,k+1} F\big(\hat{h}^P(t_j)\big),$$

where the weights $a_{j,k+1}$ are defined in (6).

Rational approximation of the Heston solution

- The Adams scheme presented above for solving the rough Heston fractional differential equation is slow!
- In [GR19], we showed how to approximate the solution of the rough Heston fractional Riccati equation by a rational function.
  - This approximation solution is just as fast as the classical Heston solution and appears to be more accurate than the Adams scheme for any reasonable number of time steps!

Rational approximation to the rough Heston solution

Wlog, set $\nu = 1$ and $x = t$. Then the rough Heston fractional Riccati ODE (3) reads

$$
\begin{aligned}
D^\alpha h(x; a) &= -\frac{1}{2} a(a + \mathrm{i}) + \mathrm{i}\,\rho\,a\,h(x; a) + \frac{1}{2}\,h(x; a)^2 \\
&= \frac{1}{2}\,(h(x; a) - r_-)\,(h(x; a) - r_+)
\end{aligned}
$$

with

$$
A = \sqrt{a\,(a + i) - \rho^2\,a^2}; \quad r_\pm = \{-\mathrm{i}\,\rho\,a \pm A\}\,.
$$

The idea is to paste together short- and long-time expansions of the solution using a rational (Padé) approximation.

Short-time expansion

From (for example) the exponentiation theorem of [AGR2020], $h(x; a)$ can be written as

$$h(x; a) = \sum_{j=0}^{\infty} \frac{\Gamma(1 + j\,\alpha)}{\Gamma(1 + (j+1)\,\alpha)} \beta_j(a)\, x^{(j+1)\,\alpha}$$

with

$$\beta_0(a) = -\frac{1}{2}\, a(a + \mathrm{i})$$

$$\beta_k(a) = \frac{1}{2} \sum_{i,j=0}^{k-2} \mathbb{1}_{\{i+j=k-2\}}\, \beta_i(a)\, \beta_j(a) \frac{\Gamma(1 + i\,\alpha)}{\Gamma(1 + (i+1)\,\alpha)}\, \frac{\Gamma(1 + j\,\alpha)}{\Gamma(1 + (j+1)\,\alpha)}$$

$$+ \mathrm{i}\, \rho\, a\, \frac{\Gamma(1 + (k-1)\,\alpha)}{\Gamma(1 + k\,\alpha)} \beta_{k-1}(a).$$

Solving the rough Heston Riccati equation for long times

- In analogy with the classical Heston solution, we expect that for a suitable range of a,

$$\lim_{x \to \infty} h(x; a) = r_-.$$

- In that case, for large x, we could linearize the fractional Riccati equation as follows.

$$
\begin{aligned}
D^\alpha h(x; a) &= \frac{1}{2} \left(h(x; a) - r_- \right) \left(h(x; a) - r_+ \right) \\
&\approx -\frac{1}{2} \left(r_+ - r_- \right) \left(h(x; a) - r_- \right) \\
&= -A \left(h(x; a) - r_- \right).
\end{aligned}
$$

continued...

- The above linear fractional differential equation has the exact solution

$$h_\infty(a, x) = r_- \left[1 - E_\alpha(-A x^\alpha)\right],$$

where $E_\alpha(\cdot)$ is the Mittag-Leffler function.

- As $x \to \infty$,

$$E_\alpha(-A x^\alpha) = -\frac{1}{A} \frac{x^{-\alpha}}{\Gamma(1 - \alpha)} + \mathcal{O}\left(|A x^\alpha|^{-2}\right).$$

- Thus, as $x \to \infty$,

$$h_\infty(a, x) - r_- = \frac{r_-}{A} \frac{x^{-\alpha}}{\Gamma(1 - \alpha)} + \mathcal{O}\left(|A x^\alpha|^{-2}\right).$$

Large x expansion

- The form of the asymptotic solution motivates the following expansion of h for large x:

$$h(x; a) = r_- \sum_{k=0}^{\infty} \gamma_k \frac{x^{-k\alpha}}{A^k \Gamma(1 - k\alpha)}.$$

- The coefficients γ_k satisfy the recursion

$$\gamma_1 = -\gamma_0 = -1$$
$$\gamma_k = -\gamma_{k-1} + \frac{r_-}{2A} \sum_{i,j=1}^{\infty} \mathbb{1}_{\{i+j=k\}} \gamma_i \gamma_j \frac{\Gamma(1 - k\alpha)}{\Gamma(1 - i\alpha) \Gamma(1 - j\alpha)}.$$

Rational approximation

- Now we have small- and large-x expansions we can compute global rational approximations to $h(x; a)$ of the form

$$h^{(m,n)}(x; a) = \frac{\sum_{i=1}^{m} p_m y^m}{\sum_{j=0}^{n} q_n y^n}$$

  with $y = x^\alpha$ that match these expansions up to order m and n respectively.

- Only the diagonal approximants $h^{(n,n)}$ are admissible approximations of h.

$h^{(3,3)}$ is the best

- From various numerical experiments, the particular approximation $h^{(3,3)}$ seems to be amazingly close to the true solution for reasonable choices of model parameters.
- Though the excellent quality of the global approximation $h^{(3,3)}$ might at first seem very surprising, it is consistent with many Padé approximation stories from the literature.
- In our case, $h^{(3,3)}$ is clearly better than either $h^{(2,2)}$ or $h^{(4,4)}$.
  - $h^{(5,5)}$ is another very good approximation, but still not as good as $h^{(3,3)}$. $h^{(5,5)}$ is obviously also slower to compute.
  - Higher order approximations may turn out to beat $h^{(3,3)}$. However, $h^{(3,3)}$ may still be best in practice if speed of computation is taken into account.

Computing $h^{(3,3)}$

- We have the series expansion of h for small y:

$$h_s(y) = b_1\, y + b_2\, y^2 + b_3\, y^3 + \mathcal{O}(y^4).$$

- We have the series expansion of h for large y:

$$h_\ell(y) = g_0 + \frac{g_1}{y} + \frac{g_2}{y^2} + \mathcal{O}\left(\frac{1}{y^3}\right).$$

- Matching the coefficients of the rational approximation

$$h^{(3,3)}(y) = \frac{p_1\, y + p_2\, y^2 + p_3\, y^3}{1 + q_1\, y + q_2\, y^2 + q_3\, y^3}$$

  to $h_s(y)$ and $h_\ell(y)$ respectively gives a linear system of six equations for the six unknowns $\{p_i, q_i\}$.

Model parameters

- Recall that in our formulation of the rough Heston model,

$$\kappa(\tau) = \frac{\nu}{\Gamma(\alpha)} \, \tau^{\alpha-1},$$

with $\alpha = H + 1/2$.

- We choose model parameters roughly consistent with those found from calibration to SPX options on May 19, 2017 in [EGR19]:

$$\xi(u) = 0.025; \ H = 0.05; \ \nu = 0.4; \ \rho = -0.65. \qquad (7)$$
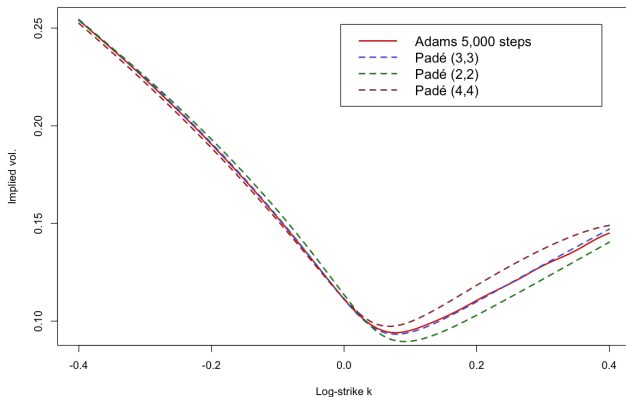
Adams and Padé smiles compared

Figure 1: The red curve is the Adams smile with 5,000 steps. $h^{(3,3)}$ is uncannily good.
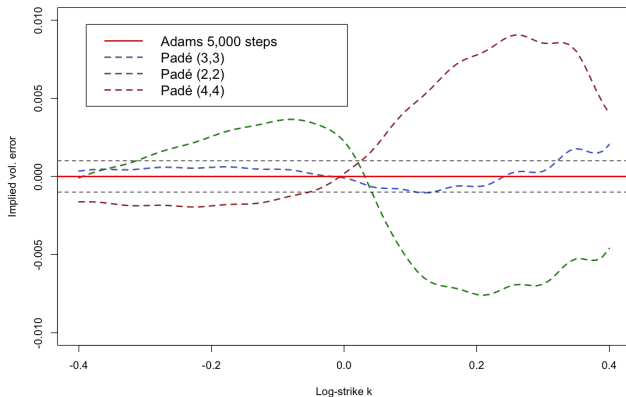
Padé vs Adams smile errors

Figure 2: The red curve is the Adams smile with 5,000 steps. Again, $h^{(3,3)}$ errors are uncannily small.

Simulation

- We now turn our attention to simulation of AFV models as prescribed in [Gat21].
- Inspired by [BLP17] and [And08] we propose two algorithms to simulate AFV models.
  - Now that we have two alternative methods of computing the volatility smile under rough Heston, we can easily check convergence of these algorithms.

Discretization of the spot and variance processes

From the AFV dynamics,

$$d\xi_t(u) = \kappa(u - t)\sqrt{v_t}\,dW_t,$$

it follows that

$$
\begin{aligned}
v_T = \xi_T(T) &= \xi_0(T) + \int_0^T d\xi_s(T) \\
&= \xi_0(T) + \int_0^T \kappa(T - s)\sqrt{v_s}\,dW_s. \quad (8)
\end{aligned}
$$

- Wlog, let $t = 0$ and $\xi(u) = \xi_0(u)$. Let the time step $\Delta = T/N$ where N is the number of steps.

- As in [BLP17], we have the following exact decomposition of (8):

$$v_{n\Delta} = \xi(n\Delta) + \sum_{k=1}^{n} \int_{(k-1)\Delta}^{k\Delta} \kappa(n\Delta - s)\sqrt{v_s}\, dW_s.$$

Discretization of the v-process

- With simpler notation,

$$v_n = \xi_n + \sum_{k=1}^{n} \int_{(k-1)\Delta}^{k\Delta} \kappa(n\Delta - s) \sqrt{v_s}\, dW_s =: \hat{\xi}_n + u_n, \quad (9)$$

where the $\mathcal{F}_{n-1}$-adapted variable $\hat{\xi}_n$ is given by

$$\hat{\xi}_n = \mathbb{E}\left[v_n | \mathcal{F}_{n-1}\right] = \xi_n + \sum_{k=1}^{n-1} \int_{(k-1)\Delta}^{k\Delta} \kappa(n\Delta - s) \sqrt{v_s}\, dW_s, \quad (10)$$

and the martingale increment u_n by

$$u_n = \int_{(n-1)\Delta}^{n\Delta} \kappa(n\Delta - s) \sqrt{v_s}\, dW_s. \quad (11)$$

The X-process

- We also need to simulate the nth increment of the component of the log-stock price process $X = \log S$ parallel to the volatility process[1],

$$\chi_n = \int_{(n-1)\Delta}^{n\Delta} \sqrt{v_s} \, dW_s. \tag{12}$$

- We then have the following discretization of the X process:

$$X_n = X_{n-1} - \tfrac{1}{4}\left(v_n + v_{n-1}\right)\Delta + \sqrt{1-\rho^2}\,\sqrt{\bar{v}_n\,\Delta}\,Z_n^\perp + \rho\,\chi_n,$$

where $Z_n^\perp$ is standard normal, independent of χ_n and u_n.

---

[1]We write the increments as χ_n to emphasize that they should be approximately χ^2 distributed random variables.

Choice of kernel

- In our computations we will focus on the *power-law* kernel:

$$\kappa(\tau) = \sqrt{2H}\,\eta\,\tau^{\alpha-1} =: \tilde{\eta}\,\tau^{\alpha-1}. \tag{13}$$

- We also need

Definition

For $i, j \geq 0$,

$$\mathcal{K}_i(\Delta) = \int_0^\Delta \kappa(s + i\Delta)\,ds;$$

$$\mathcal{K}_{i,j}(\Delta) = \int_0^\Delta \kappa(s + i\Delta)\,\kappa(s + j\Delta)\,ds.$$

- The $\mathcal{K}_{i,j}(\Delta)$ with $i \neq j$ are not in general computable in closed-form but are easy to compute numerically.

Covariances and correlations

- It can be shown that

$$\mathrm{var}[u_n|\mathcal{F}_{n-1}] = \bar{v}_n\,\mathcal{K}_{0,0}(\Delta) + \mathcal{O}\left(\Delta^{1+2H}\right), \qquad (14)$$

where

$$\bar{v}_n := \frac{1}{2H+1}\,\left[\hat{\xi}_n + 2H\,v_{n-1}\right].$$

- Similarly

$$\begin{aligned}
\mathrm{var}[\tilde{\xi}_{n+1}|\mathcal{F}_{n-1}] &\approx \bar{v}_n\,\mathcal{K}_{1,1}(\Delta) \\
\mathrm{var}[\chi_n|\mathcal{F}_{n-1}] &\approx \bar{v}_n\,\Delta \\
\mathrm{cov}[u_n,\tilde{\xi}_{n+1}|\mathcal{F}_{n-1}] &\approx \bar{v}_n\,\mathcal{K}_{0,1}(\Delta) \\
\mathrm{cov}[u_n,\chi_n|\mathcal{F}_{n-1}] &\approx \bar{v}_n\,\mathcal{K}_0(\Delta) \\
\mathrm{cov}[\chi_n,\tilde{\xi}_{n+1}|\mathcal{F}_{n-1}] &\approx \bar{v}_n\,\mathcal{K}_1(\Delta).
\end{aligned} \qquad (15)$$

Given a suitable kernel, all of these may be easily computed.

The correlation matrix

- Because variances and covariances in an AFV model are linear in ξ, the correlation matrix takes the simple form.

$$R = \begin{pmatrix} 1 & \rho_{u\chi} & \rho_{u\xi} \\ \rho_{u\chi} & 1 & \rho_{\xi\chi} \\ \rho_{u\xi} & \rho_{\xi\chi} & 1 \end{pmatrix}. \tag{16}$$

where

$$\begin{aligned}
\rho_{u\chi} &= \frac{\mathcal{K}_0(\Delta)}{\sqrt{\Delta}\sqrt{\mathcal{K}_{0,0}(\Delta)}} \\
\rho_{u\xi} &= \frac{\mathcal{K}_{0,1}(\Delta)}{\sqrt{\mathcal{K}_{0,0}(\Delta)}\sqrt{\mathcal{K}_{1,1}(\Delta)}} \\
\rho_{\xi\chi} &= \frac{\mathcal{K}_1(\Delta)}{\sqrt{\Delta}\sqrt{\mathcal{K}_{1,1}(\Delta)}}
\end{aligned}$$

are all independent of n.

The power-law kernel

- In the case of the power-law kernel $\kappa(\tau) = \tilde{\eta}\,\tau^{\alpha-1}$, these correlations are functions of H only.
- Specifically

$$\rho_{u\chi} = \frac{\sqrt{2H}}{H+1/2},$$

  and the other correlations may be easily computed numerically.

- In Figure 3, we plot these correlations as a function of H.

Plot of the correlation matrix in the power-law kernel case
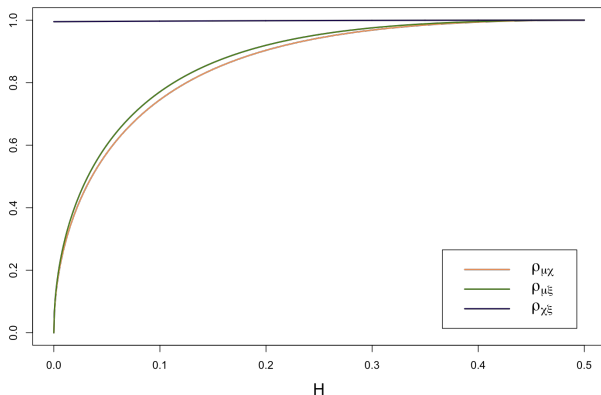

Figure 3: The correlations $\rho_{u\chi}$, $\rho_{u\xi}$, and $\rho_{\xi\chi}$ vs. H in the power-law kernel case.

A further approximation

- By assumption, the kernel behaves as a power-law kernel for Δ sufficiently small.
- Figure 3 thus suggests the following approximation whose motivation is easy to see by thinking of $\mathcal{K}_i(\Delta)$ as Δ times the average value of $\kappa(s + i\Delta)$ over the interval $(0, \Delta]$.

Approximate covariance

For $i \geq 0$ and $j \geq 1$,

$$\mathcal{K}_{i,j}(\Delta)\, \Delta \approx \mathcal{K}_i(\Delta)\, \mathcal{K}_j(\Delta). \tag{17}$$

An approximate correlation matrix

With the approximation (17),

$$\mathcal{K}_{0,1}(\Delta) \approx \frac{1}{\Delta}\, \mathcal{K}_1(\Delta)\, \mathcal{K}_0(\Delta); \quad \mathcal{K}_{1,1}(\Delta) \approx \frac{1}{\Delta}\, \mathcal{K}_1(\Delta)^2.$$

Substituting these expressions into (15) gives the correlation matrix

$$\bar{R} = \left(\begin{array}{ccc} 1 & \bar{\rho} & \bar{\rho} \\ \bar{\rho} & 1 & 1 \\ \bar{\rho} & 1 & 1 \end{array} \right), \tag{18}$$

where

$$\bar{\rho} \approx \frac{\mathcal{K}_0(\Delta)}{\sqrt{\mathcal{K}_{0,0}(\Delta)\, \Delta}} = \rho_{u\,\chi}.$$

Consequences for simulation

- At each step, we need to generate (at least) three random variables: u_n, χ_n, and $\hat{\xi}_{n+1}$.

$$
\begin{aligned}
u_n &= \int_{(n-1)\Delta}^{n\Delta} \kappa(n\Delta - s)\sqrt{v_s}\, dW_s \\
\chi_n &= \int_{(n-1)\Delta}^{n\Delta} \sqrt{v_s}\, dW_s \\
\hat{\xi}_{n+1} &= \xi_{n+1} + \sum_{k=1}^{n} \int_{(k-1)\Delta}^{k\Delta} \kappa((n+1)\Delta - s)\sqrt{v_s}\, dW_s.
\end{aligned}
$$

- When the model is Markovian ($H = 1/2$), we need only generate u_n at the nth time step; χ_n and $\hat{\xi}_{n+1}$ are perfectly correlated with u_n.
  - In practice, in the non-Markovian case ($H < 1/2$), we need only generate one other random variable consistent with the correlation matrix $\bar{R}$.

Average values of the kernel

- Echoing the notation of [BLP17], let

$$b_j^{\star 2} = \frac{1}{\Delta} \, \mathcal{K}_{j-1,j-1}(\Delta). \tag{19}$$

- $b_j^{\star 2}$ thus gives the RMS average of the kernel at the jth lag.

The evolution of the forward variance curve

- The approximation

$$\int_{(k-1)\Delta}^{k\Delta} \kappa((n+1)\Delta - s)\sqrt{v_s}\,dW_s \;\approx\; b_{n+1-k}^\star\,\chi_k$$

gives

$$\hat{\xi}_{n+1} \;\approx\; \xi_{n+1} + \sum_{k=1}^n b_{n+1-k}^\star\,\chi_k.$$

- Similarly (though not needed for the algorithm), for $m > n$,

$$\mathbb{E}\left[\,v_m\,|\,\mathcal{F}_n\right] \;\approx\; \xi_m + \sum_{k=1}^n b_{m-k}^\star\,\chi_k.$$

- We see that the entire forward variance curve evolves according to the weighted historical path of the $X = \log S$ process.

The Andersen Quadratic Exponential (QE) scheme

- Naïve simulation of the v process leads to negative values
- Andersen's Quadratic Exponential (QE) scheme [And08] guarantees v positive
    - Conditional means and variances are matched at each step
- We simulate according to the value of the ratio

$$\psi_n := \frac{\text{var}[v_n|\mathcal{F}_{n-1}]}{\hat{\xi}_n^2} = \frac{\text{var}[u_n|\mathcal{F}_{n-1}]}{\hat{\xi}_n^2}. \tag{20}$$

The Andersen Quadratic Exponential (QE) scheme

- If $\psi_n \leq 2$, simulate v_n as

$$v_n = \alpha_n \left(\beta_n + Z_n\right)^2$$

with $Z_n \sim N(0,1)$ and

$$\beta_n^2 = \frac{2}{\psi_n} - 1 + \sqrt{\frac{2}{\psi_n}} \sqrt{\frac{2}{\psi_n} - 1}; \quad \alpha_n = \frac{\hat{\xi}_n}{1 + \beta_n^2}.$$

- On the other hand, if $\psi_n \geq 1$, simulate v_n as

$$v_n = -\mathbb{1}_{\{U_n < p_n\}} \, \gamma_n \, \log \frac{U_n}{p_n}$$

with $U_n \sim \mathcal{U}(0,1)$ and

$$p_n = \frac{2}{1 + \psi_n}; \quad \gamma_n = \frac{1}{2} \hat{\xi}_n \left(1 + \psi_n\right).$$

Conditional means and variances

- It is straightforward to check that means and variances are correctly matched in both cases.
- Since the two regions of applicability overlap, Andersen suggests to use algorithm ψ^- if $\psi_n < 3/2$ and algorithm ψ^+ if $\psi_n \geq 3/2$.

A Riemann-sum QE scheme

- Inspired by the Riemann-sum scheme of [BLP17] and the rough-Donsker scheme of [HJM17], we simulate the u_n, $\hat{\tilde{\xi}}_{n+1}$ and χ_n as if all three were perfectly correlated, equivalent to setting $\bar{\rho} = 1$ in (18).
  - From Figure 3 such an approximation may be justified if H is not too much less than $\frac{1}{2}$.

The RSQE scheme

> ### The RSQE scheme
>
> 1. Given χ_k, for $k < n$, with ϵ very small, compute
> $\hat{\xi}_n = \max\left[\epsilon,\; \xi_n + \sum_{k=1}^{n-1} b_{n-k+1}^{\star}\, \chi_k\right]$.
>
> 2. With $\mathrm{var}[v_n|\mathcal{F}_{n-1}] = b_1^{\star 2}\, \bar{v}_n\, \Delta$, simulate v_n using the QE scheme.
>
> 3. $u_n = v_n - \hat{\xi}_n$.
>
> 4. $\chi_n = \frac{u_n}{b_1^{\star}}$.
>
> 5. Finally,
> $X_n = X_{n-1} - \frac{1}{4}\left(v_n + v_{n-1}\right)\Delta + \sqrt{1-\rho^2}\,\sqrt{\bar{v}_n\, \Delta}\, Z_n^{\perp} + \rho\, \chi_n.$

A hybrid QE scheme

- The RSQE scheme matches unconditional means and variances at each step but it does not match the covariance structure of the process.
- For example, consider the conditional covariance between u_n and χ_n which is given by

$$\text{cov}[u_n, \chi_n | \mathcal{F}_{n-1}] = \int_{(n-1)\Delta}^{n\Delta} \kappa(n\Delta - s) \, \mathbb{E}\left[v_s | \mathcal{F}_{n-1}\right] \, ds \approx \bar{v}_n \, \mathcal{K}_0(\Delta).$$

- The RSQE scheme sets $u_n = b_1^\star \chi_n$ so that

$$\text{cov}[u_n, \chi_n | \mathcal{F}_{n-1}] \approx b_1^\star \, \text{var}[\chi_n | \mathcal{F}_{n-1}] = \bar{v}_n \, \sqrt{\mathcal{K}_{0,0}(\Delta) \, \Delta},$$

which is equivalent to the approximation

$$\mathcal{K}_0(\Delta) \approx \sqrt{\mathcal{K}_{0,0}(\Delta) \, \Delta}. \tag{21}$$

- Approximation (21), though accurate for small Δ when the kernel κ has no singularity at zero, is obviously very inaccurate when H is small.
- The essence of the hybrid scheme with $\kappa = 1$ of [BLP17] is to correct the error in the approximation (21) by simulating another random variable, uncorrelated with u_n, so as to match the covariance of u_n and χ_n.
  - For this, we need a bivariate version of Andersen's QE scheme.

A bivariate version of Andersen's QE scheme

- As before, let

$$u_n = \int_{(n-1)\Delta}^{n\Delta} \kappa(n\Delta - s)\sqrt{v_s}\,dW_s; \quad \chi_n = \int_{(n-1)\Delta}^{n\Delta} \sqrt{v_s}\,dW_s.$$

- Linear regression gives

$$u_n \approx \beta_{u\chi}\,\chi_n + \varepsilon_n,$$

  where $\beta_{u\chi} = \mathcal{K}_0(\Delta)/\Delta$, and ε_n and χ_n are uncorrelated.

- Since $v_n = \hat{\xi}_n + u_n \geq 0$, we must ensure that
  $\beta_{u\chi}\,\chi_n + \varepsilon_n + \hat{\xi}_n \geq 0$.

- A scheme to achieve this is given in the following lemma.

A bivariate QE scheme

Lemma 2

Let χ_n and ε_n be generated independently using the QE scheme with the following conditional means and variances:

$$\mathbb{E}\left[\beta_{u\chi}\chi_n|\mathcal{F}_{n-1}\right] = \tfrac{1}{2}\hat{\xi}_n; \quad \mathbb{E}\left[\varepsilon_n|\mathcal{F}_{n-1}\right] = \tfrac{1}{2}\hat{\xi}_n;$$
$$\mathrm{var}[\chi_n|\mathcal{F}_{n-1}] = \bar{v}_n\,\Delta; \quad \mathrm{var}[\varepsilon_n|\mathcal{F}_{n-1}] = \bar{v}_n\left(\mathcal{K}_{0,0}(\Delta) - \tfrac{1}{\Delta}\mathcal{K}_0(\Delta)^2\right).$$

Then $v_n = \beta_{u\chi}\chi_n + \varepsilon_n + \hat{\xi}_n \geq 0$. Moreover, with $u_n = \beta_{u\chi}\chi_n + \varepsilon_n$,

$$\mathrm{var}[u_n|\mathcal{F}_{n-1}] = \bar{v}_n\,\mathcal{K}_{0,0}(\Delta); \quad \mathrm{cov}[u_n, \chi_n|\mathcal{F}_{n-1}] = \bar{v}_n\,\mathcal{K}_0(\Delta).$$

The hybrid QE (HQE) scheme

The HQE scheme

1. Given χ_k, for $k < n$, with ϵ very small, compute
   $\hat{\xi}_n = \max\left[\epsilon, \xi_n + \sum_{k=1}^{n-1} b_{n-k+1}^\star \chi_k\right]$.

2. Simulate χ_n and ε_n using the bivariate QE scheme

3. $v_n = \hat{\xi}_n + \frac{1}{\Delta}\mathcal{K}_0(\Delta)\,\chi_n + \varepsilon_n$.

4. Finally,
   $X_n = X_{n-1} - \frac{1}{4}\left(v_n + v_{n-1}\right)\Delta + \sqrt{1-\rho^2}\,\sqrt{\bar{v}_n\,\Delta}\,Z_n^\perp + \rho\,\chi_n$.

Rough Heston parameters

- Consider the power-law kernel $\kappa(\tau) = \sqrt{2H}\,\eta\,\tau^{\alpha-1}$ with parameters roughly consistent with those found from calibration to SPX options on May 19, 2017 in [EGR19]:

$$\xi(u) = 0.025; \ H = 0.05; \ \eta = 0.8; \ \rho = -0.65. \qquad (22)$$

- Note that the rough Heston kernel in [EGR19] takes the form

$$\kappa(\tau) = \frac{\tau^{\alpha-1}}{\Gamma(\alpha)},$$

so ν in in [EGR19] and η in (13) are related as $\nu = \eta\,\sqrt{2H}\,\Gamma(\alpha)$.
  - $\eta = 0.8$ corresponds to $\nu \approx 0.4089$.

Richardson extrapolation

- It seems that the order of weak convergence of the fractional Adams scheme is one.
  - It therefore makes sense to use Richardson extrapolation to increase the order of convergence.

Definition 3 (Richardson extrapolation)

Let $\mathcal{S}_n$ denote an *n*-step approximation of the volatility smile according to some numerical scheme. Then the *n-step Richardson extrapolation* is given by

$$\mathcal{S}_n^R = \mathcal{S}_{2n} - \mathcal{S}_n.$$

- Adopting the $2,500$-step Richardson extrapolated Adams smile $\mathcal{S}_{2500}^R$ as our reference smile, we plot errors in the 200 step Adams and Padé approximated smiles in Figure 4.
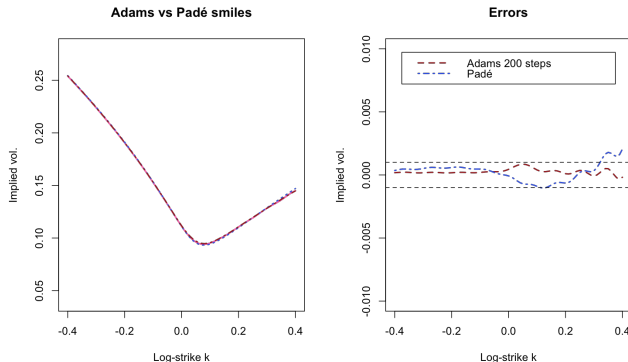
Plots of smile and errors

Figure 4: The 1-year rough Heston smile with parameters (22). The pink curve is the reference Adams smile S_{2500}^R. The blue and brown curves are from the Adams scheme with 200 steps and the Padé approximation respectively. The dashed horizontal lines indicate our target error band of $\pm 0.10\%$.
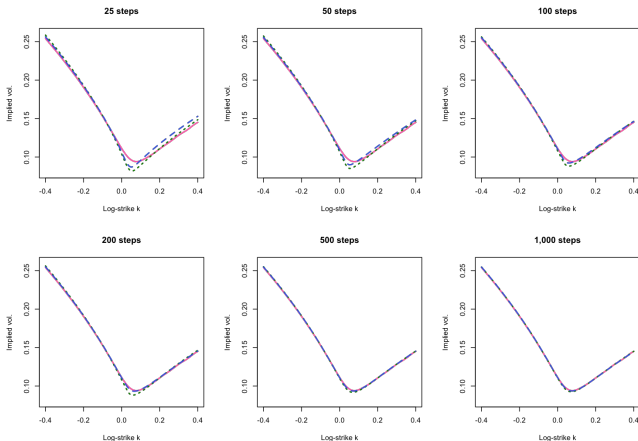
Convergence of the RSQE and HQE schemes

Figure 5: The 1-year rough Heston smile with parameters (22). The pink reference curve is the Adams reference smile $\mathcal{S}_{2500}^{R}$. The green-dotted and blue-dashed curves are from RSQE and HQE simulations with 10^6 paths.
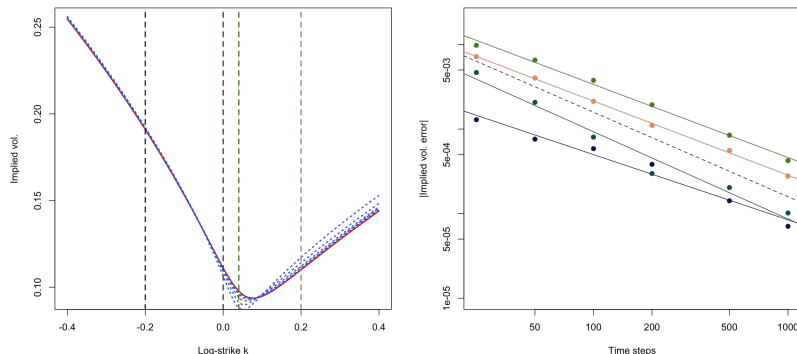
Convergence of the HQE scheme

Figure 6: In the LH plot, the pink curve is the HQE smile $\mathcal{S}_{500}^{R}$. The blue dotted lines are HQE smiles S_n computed with $n \in \{25, 50, 100, 200, 500, 1000\}$. In the RH plot, we plot absolute implied volatility errors. All simulations are with 10^6 paths.

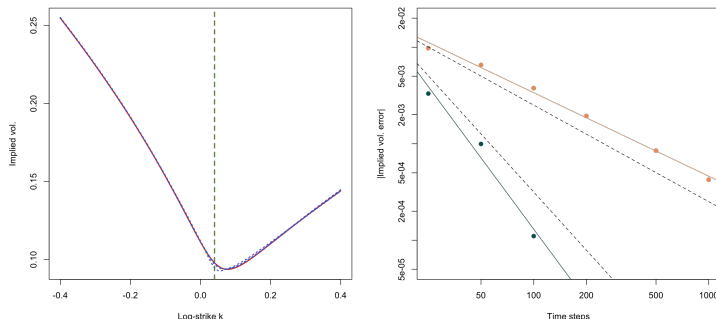# Convergence of Richardson extrapolated HQE smiles

Figure 7: In the LH plot, the pink curve is the HQE smile $\mathcal{S}_{500}^R$. The blue dotted lines are the Richardson-extrapolated smiles S_n^R computed with $n \in \{25, 50, 100\}$. In the RH plot, we plot absolute implied volatility errors vs time steps for log-strike $k = 0.04$. We see evidence of order 2 weak convergence of Richardson-extrapolated smiles.

Summary

- We now have two ways to compute European option prices in AFV models: the Adams scheme and simulation using the HQE scheme.
    - In the special case of the rough Heston model with $\lambda = 0$, we also have the rational approximation.
- For other more exotic options, we only have simulation.
- The HQE scheme is as fast as the Adams scheme for a similar level of accuracy.
    - Moreover, there are many ways to potentially increase the efficiency of the HQE scheme (FFT and variance reduction for example).

References

Eduardo Abi Jaber, Martin Larsson, and Sergio Pulido
Affine Volterra processes
The Annals of Applied Probability, 29(5):3155–3200, 2019.

Elisa Alòs, Jim Gatheral, and Radoš Radoičić.
Exponentiation of conditional expectations under stochastic volatility.
Quantitative Finance, 20(1):13–27, 2020.

Leif Andersen.
Simple and efficient simulation of the Heston stochastic volatility model.
The Journal of Computational Finance, 11(3):1–42, 2008.

Fabio Baschetti, Giacomo Bormetti, Siliva Romagnoli, and Pietro Rossi.
The SINC way: A fast and accurate approach to Fourier pricing.
Quantitative Finance, available online, 2021.

Lorenzo Bergomi and Julien Guyon.
Stochastic volatility's orderly smiles.
Risk May, pages 60–66, 2012.

Mikkel Bennedsen, Asger Lunde, and Mikko S Pakkanen.
Hybrid scheme for Brownian semistationary processes.
Finance and Stochastics, 21(4): 931-965, 2017.

Kai Diethelm, Neville J. Ford, and Allan D. Freed

Detailed error analysis for a fractional Adams method.
Numerical Algorithms, 36(1) 31–52, 2004.

Omar El Euch and Mathieu Rosenbaum.

The characteristic function of rough Heston models.
Mathematical Finance, 29(1) 3–38, 2019.

Omar El Euch, Jim Gatheral, and Mathieu Rosenbaum.

Roughening Heston
Risk.net, May 2019.

F. Fang and C. W. Oosterlee,

A Novel Pricing Method for European Options Based on Fourier-Cosine Series Expansions.
SIAM Journal on Scientific Computing, 31(2) 826–848, 2009.

Peter K Friz, Jim Gatheral and Radoš Radoičić.

Forests, cumulants, martingales.
arXiv:2002.01448, 2020.

Masaaki Fukasawa.

The normalizing transformation of the implied volatility smile.
Mathematical Finance, 22(4):753–762, 2012.

Masaaki Fukasawa.

Volatility derivatives and model-free implied leverage.
International Journal of Theoretical and Applied Finance, 17(01):1450002, 2014.

Jim Gatheral.
The volatility surface: A practitioner's guide.
John Wiley & Sons, 2006.

Jim Gatheral and Martin Keller-Ressel.
Affine forward variance models.
Finance and Stochastics, 23(3):501–533, 2019.

Jim Gatheral and Radoš Radoičić.
Rational approximation of the rough Heston solution.
International Journal of Theoretical and Applied Finance, 22(3):1950010–19, 2019.

Jim Gatheral
Efficient simulation of affine forward variance models.
SSRN, https://www.ssrn.com/abstract=3876680, 2021.

Blanka Horvath, Antoine Jacquier, and Aitor Muguruza.
Functional central limit theorems for rough volatility.
SSRN, https://www.ssrn.com/abstract=3078743, 2017.

Alan Lewis,
Option Valuation under Stochastic Volatility with Mathematica Code.
Finance Press: Newport Beach, CA, 2000.